Kinetic study of steam gasification of biomass chars in a fluidized bed reactor

Mathieu MORIN[1*], Sébastien PECATE[1], Mehrdji HEMATI[1], Enrica MASI[2]

[1]Laboratoire de Génie Chimique
4 Allée Emile Monso - 31432 Toulouse
[2]Institut de Mécanique des Fluides de Toulouse
Allée Professeur Camille Soula - 31400 Toulouse
[*](corresponding author: mathieu.morin@ensiacet.fr)

Résumé - Ce travail est consacré à l'étude cinétique de la vapogazéification en réacteur à lit fluidisé de chars issus de la pyrolyse rapide de bâtonnet de bois d'hêtre. L'effet de la température entre 700 et 850°C et de la pression partielle de la vapeur d'eau entre 10130 et 70910 Pa sont particulièrement étudiés. Les résultats expérimentaux sont confrontés à différents modèles cinétiques de réaction gaz-solide. Parmi eux, le modèle du noyau rétrécissant prédit de manière satisfaisante l'ensemble des résultats expérimentaux. Les paramètres cinétiques (constante pré-exponentielle, énergie d'activation Ea et ordre de la réaction par rapport à la vapeur d'eau) ont été déterminés en se plaçant dans les conditions opératoires où la réaction chimique est l'étape limitante.

1. Introduction

Biomass gasification is a promising alternative to fossil fuels for the synthesis of highly energetic products via Fischer-Tropsch or methanation processes. It is a thermochemical conversion occurring at high temperatures with many simultaneous reactions. For temperatures above 350°C, biomass undergoes a thermal decomposition called pyrolysis which leads to the formation of volatile products either condensable (steam and tars) or non-condensable (H_2, CO, CO_2, CH_4 and C_2H_x) and a solid residue called char [1]. Then, the char reacts with steam and carbon dioxide at temperatures greater than 700°C to produce syngas. These transformations are endothermic. Therefore, a contribution of energy is required to maintain the temperature and the different reactions. One of the most encouraging and advanced technology is dual fluidized beds [2]. Its principle relies on the circulation of a media (sand, olivine or catalyst particles) which acts as a heat carrier between an endothermic reactor, where biomass gasification produces syngas, and an exothermic reactor where combustion of a part of the char from the gasification of biomass produces heat. Therefore, it is of importance to carefully understand the effect of operating conditions on char structure and composition which are directly related to its reactivity in combustion and steam gasification. Besides, a thorough determination of kinetic parameters of steam gasification and combustion of char is needed in order to design these types of processes.

During pyrolysis of biomass, many changes occur in the solid structure. These changes are responsible for the steam gasification and combustion reactivity of the chars. For instance, in our previous works [3], we found that an increase in the pyrolysis temperature of biomass chars leads to the development of disordered structure, the decrease in hydrogen and oxygen contents and the raise in the aromaticity nature of the char. Hence, raising pyrolysis temperature decreases the reactivity of char both in combustion and steam gasification processes.

The amount of literature works dealing with the steam gasification of coal char is very large [4-8]. However, researches in regard with biomass char have still hardly been investigated and most of these works can be found in the review of Di Blasi [9].

In this study, the isothermal steam gasification of biomass chars is carried out in a fluidized bed reactor. Influence of temperature and partial pressure of steam is investigated. Kinetic parameters are determined and compared with results reported in the literature.

2. Experimental section

2.1. Char preparation and characterization

The biomass used in this work is beech stick (D=5 mm, L=10 mm). Fast pyrolysis of biomass was carried out in a batch fluidized bed reactor at 650°C in an inert atmosphere of nitrogen. The details of pyrolysis procedure and the char characterization can be found elsewhere [3]. The produced chars called STI650 have a cylindrical form (D=4 mm, L=10 mm). Its physical and chemical properties are presented in Table 1.

	Biomass type	*Solid form*	*Pyrolysis Temp*	*True Density*	*C*	*H*	*O*	*Ash*	*Chemical formula*
	-	-	°C	kg/m^3	db, wt%				-
Beech	Beech	Stick	-	-	44.63	6.37	45.24	3.76	$CH_{1.71}O_{0.76}$
STI650	Beech	Stick	650	1589.4	84.47	2.75	7.39	5.39	$CH_{0.39}O_{0.07}$

Table 1 : Ultimate analysis and properties of the biomass and its associated char.

2.2. Steam gasification experiments

Experimental setup: The experimental setup is shown in Figure 1(A). The fluidized bed reactor consists in a tube of internal diameter of 5.26 cm and a height of 92 cm heated by an electric furnace (height : 28 cm, inner diameter : 36 cm). Olivine is used as the fluidized solids: surface mean diameter (d_p) equal to 268 μm and apparent density (ρ_p) equal to 3020 kg/m^3. About 580 g of olivine is introduced inside the reactor. Minimum fluidization velocity of olivine was measured experimentally and is equal to 5.8 cm/s at 850°C. The reactor is supplied with N_2 and steam. The feeding gas and water are preheated between 300 and 400°C in a stainless steel tube forming a coil around the reactor before entering in the bed. The temperature inside the fluidized bed is controlled by two thermocouples placed at 5 and 25 cm above the distributor. The former is used to regulate the temperature of the reactor. A differential pressure transmitter is connected at 5 and 500 mm above the distributor in order to follow the pressure drop of the bed. After reaching the preset reactor temperature and the operating conditions, about 8.7 g of STI650 (ca. 1.5% of the mass bed) are introduced inside the reactor.

By using two thermocouples located at 5 and 15 cm above the distributor, Figure 1(B) indicates that a homogeneous temperature inside the bed and a good fluid-solid mixture are obtained for gas velocity greater than 2.5 times the minimum fluidization velocity. It can be seen from Figure 1 (C) that the axial temperature of the bed rises abruptly above the distributor and reaches a temperature of 850°C at about 3 cm above the distributor. The temperature remains constant and decrease significantly above 27 cm which is the height of the fluidized bed and the beginning of the freeboard zone.

Gas analysis: The gas sample is sucked by a vacuum pump (fixed volume flow rate of 100 mL/min at STP) and passes through a stainless mobile probe (inner diameter of 4 mm) located at the fluidized bed surface. To prevent any condensations of tar or steam, all the lines from the reactor to the entrance of the condensation system are heated to a temperature of 150°C. Gas sample passes through two wash-bottles cooled at 0°C and -20°C respectively, to condense steam and tars. A micro Gas Chromatograph (microGC) Agilent 490 is used to online analyze the non-condensable gases. Hence, quantification of N_2, H_2, O_2, CO, CH_4, CO_2

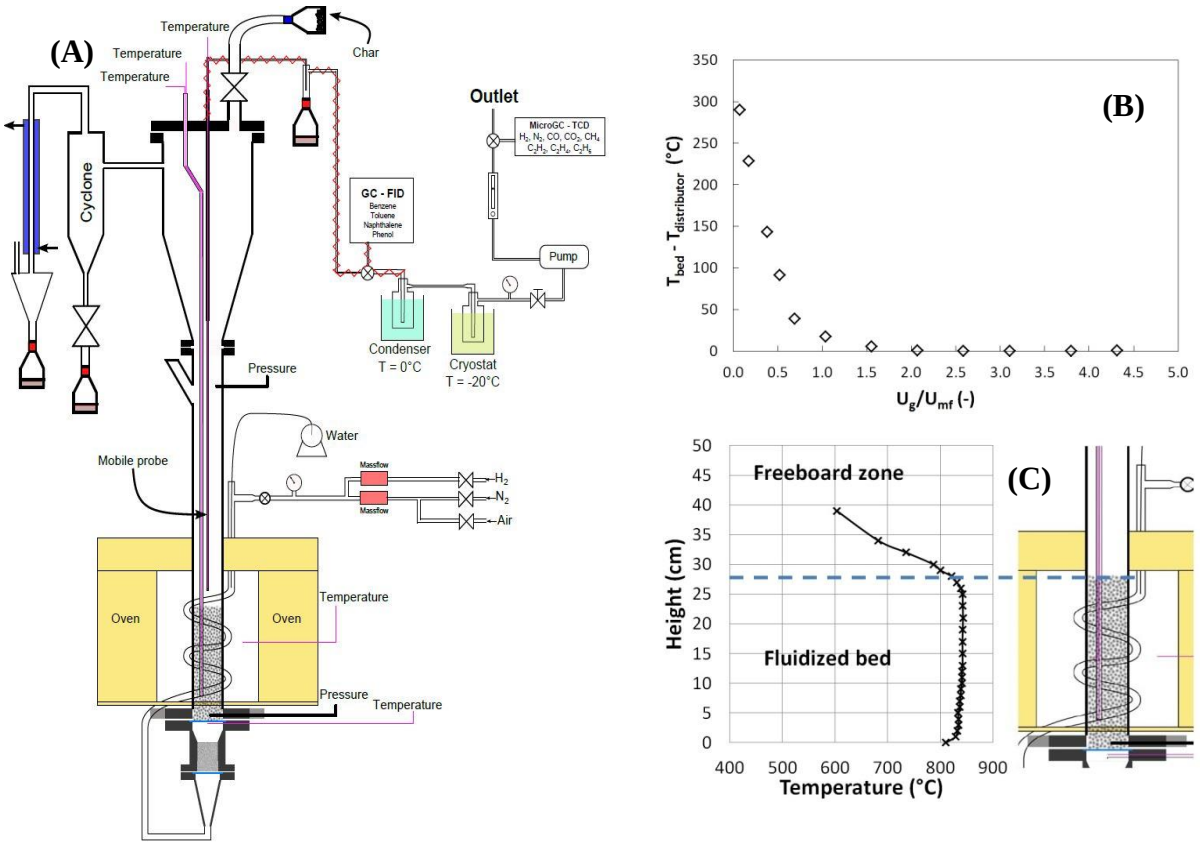

Figure 1 : (A) Schematic diagram of the fluidized bed reactor used for steam gasification of chars, (B) Temperature difference between the center and the distributor of the fluidized bed reactor, fluidization media: olivine, (C) Height of the fluidized bed versus temperature, fluidization velocity: 7.U_{mf}.

and C_2H_x is carried out. The time-lapse between two quantifications is 3 minutes.

Operating conditions and parameters of the study: The operating conditions of the different experiments are given in Table 2. The total molar flow rate was determined to keep a constant gas velocity equal to 2.5 U_{mf} and to avoid any particles elutriation. For each experiment, the composition of the non-condensable produced gases was analyzed as a function of time from the continuous Micro-GC analysis. The total molar gas flow rate at the outlet of the reactor is given by:

$$\dot{n}_t(t) = \frac{\dot{n}_{N_2}}{x_{N_2}(t)} \tag{1}$$

The carbon molar flow rate is calculated as follow:

$$\dot{n}_{carbon}(t) = \sum_{i=1}^{N_{tot}} x_i(t) \cdot \dot{n}_t(t) \cdot C_i \tag{2}$$

Carbon conversion rate and reaction rate are determined using the equations:

$$X_c = \frac{\int_{t=0}^{t_f} \dot{n}_{carbon}(t)dt}{(n_{carbon})_{char}} \quad and \quad \frac{dX_c}{dt} = \frac{\dot{n}_{carbon}(t)}{(n_{carbon})_{char}} \tag{3}$$

Where $\dot{n}_t(t)$ is the total molar flow rate, $\dot{n}_{N_2}$ the molar flow rate of nitrogen at the inlet of the reactor, $x_{N_2}(t)$ the molar fraction of nitrogen, $x_i(t)$ the molar fraction of constituent i, $\dot{n}_{carbon}(t)$ the carbon molar flow rate in time in gas stream at t, C_i the number of carbon in molecule i, $(n_{carbon})_{char}$ the number of moles of carbon in the introduced char.

Exp.	Temp.	P_{H2O}	F_{N2}	F_{H2O}	F_{Total}
-	°C	Pa	mol/min	mol/min	mol/min
1	700	30390	0.18	0.08	0.26
2	750	30390	0.17	0.07	0.24
3	800	30390	0.16	0.07	0.22
4	850	10130	0.18	0.02	0.21
5	850	30390	0.14	0.06	0.21
6	850	50650	0.10	0.10	0.21
7	850	70910	0.06	0.14	0.21

Table 2 : Operating conditions for steam gasification of STI650 in the fluidized bed reactor.

3. Results and discussion

3.1. Steam gasification of STI650

The result of a typical experiment is shown in Figure 2 (A) which presents the variation of the molar percentage of the produced gases H_2, CO, CO_2 and CH_4 during steam gasification at 850°C and 30% H_2O (exp. n°5). Nitrogen molar percentage is not shown since it only acts as a carrier gas and is not involved in the gasification reactions. Profile curves from Figure 2(A) are close to those obtained by Xu et al. [10] for biomass char steam gasification in a fixed bed reactor. These authors divided the process of gas released into three stages: an initial heat-up and slow gas production stage, a fast gas production stage and a final falling gas production stage.

In the present study, the detected components take about 10 min before reaching a maximum concentration. The origin of this maximum is not well understood yet [11]. In thermogravimetric analysis or other fixed bed reactors, some researchers [12] concluded that this maximum is due to the low gasification agent content in the reactive atmosphere just after switching the gas from inert to reactive. Consequently, the reaction rate is lower at the beginning of the reaction and progressively increases until a maximum which usually appears in the conversion range of 0.3-0.7 [12]. In our work, we attribute this maximum to the partial thermal degradation of the char occurring until a carbon conversion rate of about 0.15 according to the following reaction:

$$CH_xO_y \rightarrow \alpha CO + \beta H_2 + \gamma CO_2 + \varepsilon CH_4 + \sigma C \quad (4)$$

This stage was also highlighted by observing the fast formation of non-condensable gases during the insertion of char in the reactor in presence of nitrogen. For carbon conversion rate above 0.15, reactions (5) mainly take place as it is shown by the ratio between the molar flow rate of produced hydrogen and the sum of carbon dioxide and monoxide molar flow rate (Figure 2 (B)). It can be seen that a ratio of 1 occurs after 10 min which means that only the steam gasification of carbon and the Water-Gas-Shift reactions take place.

$$C + H_2O \rightarrow CO + H_2 \quad and \quad CO + H_2O \leftrightarrow CO_2 + H_2 \quad (5)$$

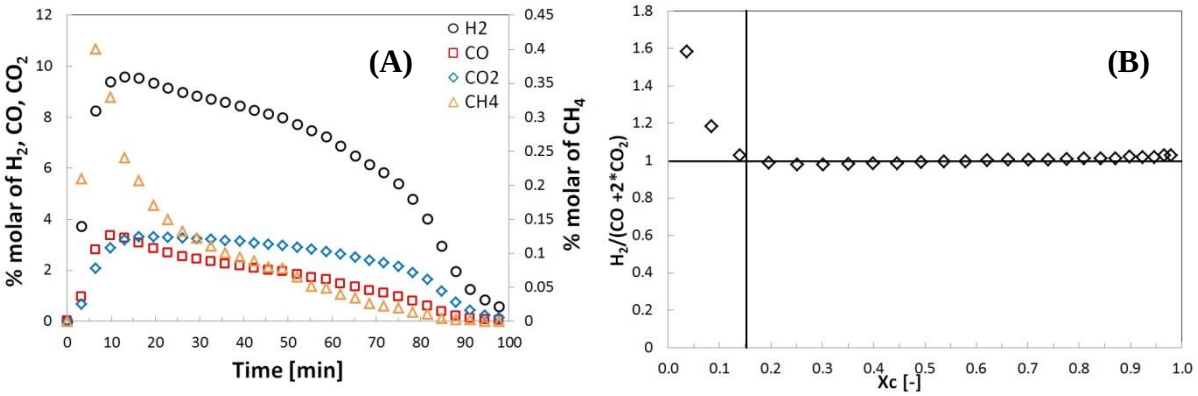

Figure 2 : Steam gasification of the char in the fluidized bed reactor at 850°C, P_{H2O} = 30390 Pa and U_g = 2.5 U_{mf}, (A) Time-dependence of the produced gas concentration (B) Molar flow rate of hydrogen over carbon monoxide and dioxide versus carbon conversion.

3.2. Effect of temperature

Figure 3(A) presents carbon conversion rate versus reaction time for different temperatures and a fixed steam partial pressure of 30390 Pa. It shows that the higher the temperature, the faster is the carbon conversion rate. This result was also observed by many previous researchers [9]. For a given carbon conversion rate (X_c = 0.4), it requires a much shorter reaction time at the higher reaction temperature (25 min, 35 min, 70 min and 180 min for temperatures of 850°C, 800°C, 750°C and 700°C respectively).

Figure 3(B) illustrates the variation of reaction rate versus conversion rate at different temperatures. It can be seen that the reaction rate increase quickly at the beginning of the gasification until a maximum. As discussed in section 3.1, this maximum is associated to the initial heat-up of the char which releases volatile products.

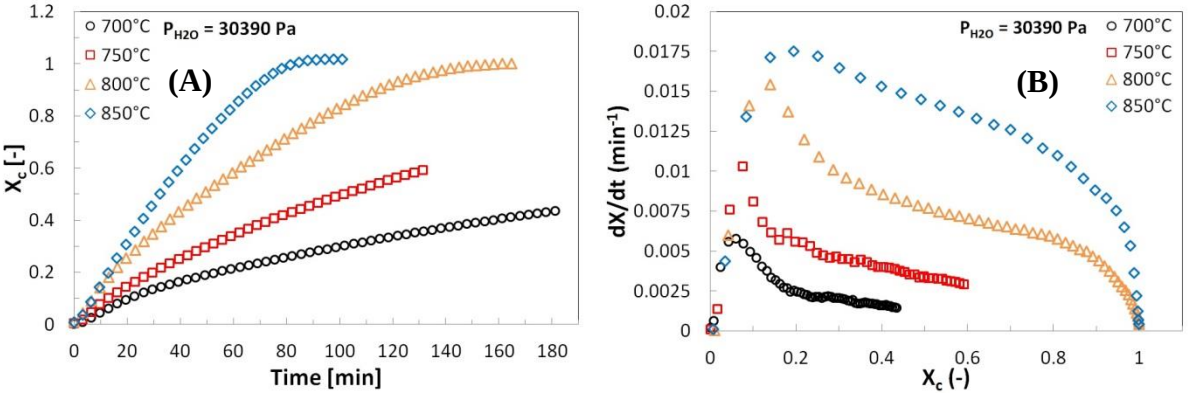

Figure 3 : Steam gasification of the char at P_{H2O} = 30390 Pa for various temperatures (A) Carbon conversion rate versus time, (B) Gasification rate versus carbon conversion rate.

Figure 4 presents a plot of $\ln(dX_c/dt)$ versus $1/T$ at a fixed conversion rate of 0.4. It can be seen that char gasification rate is highly dependent of temperature. Hence, for temperatures between 700 and 850°C, char gasification rate follows an Arrhenius expression according to Equation (6). This result shows that the reaction is controlled by chemical steps with an activation energy calculated from Figure 4 equal to 137 kJ/mol. Same observations were also found by Wang et al. [5]. According to these authors, the effects of external transfers (heat and mass) become significant for temperatures above 900°C.

$$\frac{dX_c}{dt} = A \cdot \exp\left(-\frac{E_a}{RT}\right) \cdot P_i^n \cdot f(X_c) \qquad (6)$$

Where $f(X_c)$ represents the reaction model, A is the pre-exponential factor, E_a is the activation energy, T is absolute temperature, R is the gas constant, P_i is the steam partial pressure and n stands for the apparent reaction order.

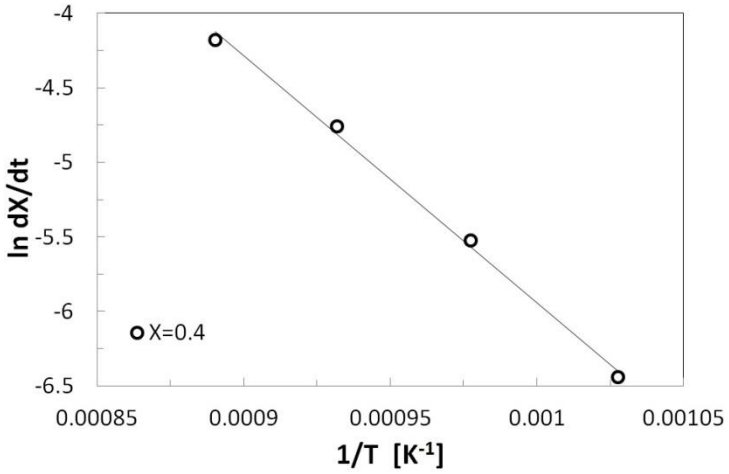

Figure 4 : Char gasification rate versus 1/T for the steam gasification of the char at various carbon conversions and a steam partial pressure of 30390 Pa.

3.3. Effect of steam partial pressure

The influence of steam partial pressure was examined at 850°C by setting the value of this factor respectively at 0.1, 0.3, 0.5 and 0.7 atm. For all experiments, the total pressure of the reactor was fixed to 1 atm. Figure 5 shows that a raise of the steam partial pressure leads to a higher gasification rate. This result is well established in literature [5]. However, this effect becomes less significant for values greater than 0.5 atm. During steam gasification of char, steam molecules are adsorbed on the active sites of char structure and react with carbon. Therefore, once the steam partial pressure is high enough, active sites are saturated and an increase in the steam content would not influence significantly the carbon conversion.

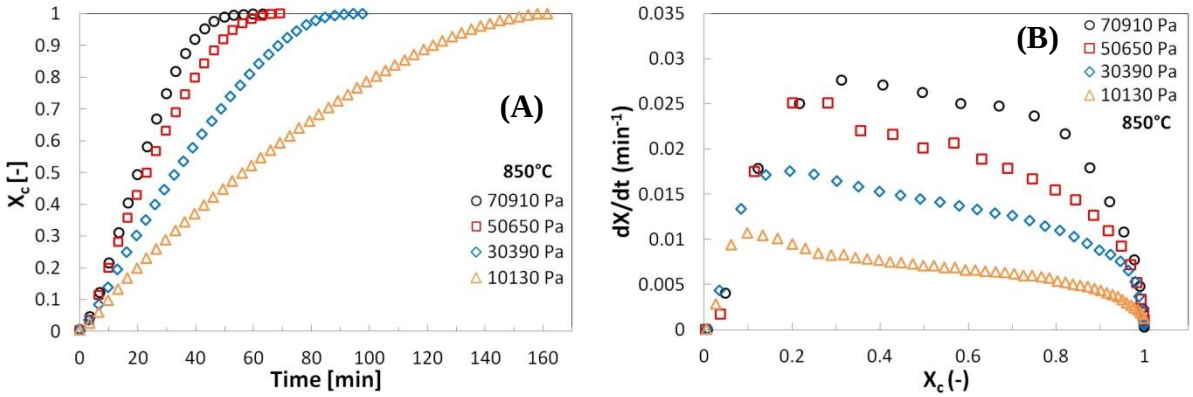

Figure 5 : Steam gasification of the char at 850°C, a total pressure of 1 atm and different steam partial pressures, (A) Carbon conversion rate versus time, (B) Gasification rate versus carbon conversion rate.

3.4. Determination of kinetic model and parameters

Several models can represent kinetics of steam gasification of chars. Three kinetic models were tested in this work: the volumetric model (VM) [6], the random pore model (RPM) [13] and the shrinking core model (SCM) [14]. In the present study, the shrinking core model (SCM) was found to best-fitted the experimental results. Hence, this model was adopted to estimate kinetic parameters. Considering a cylindrical particles having an initial radius R_0, the

reaction takes place at the outside surface of the particles in isothermal conditions. As the reaction proceeds, the surface moves into the interior of the solid leaving behind an inert ash having the same initial radius R_0 [14]. By assuming a steady-state and a chemical reaction control, the reaction rate can be expressed as:

$$\frac{dX_c}{dt} = A \cdot \exp\left(-\frac{E_a}{RT}\right) \cdot P_i^n \cdot (1 - X_c)^{1/2} \quad (7)$$

For fixed values of P_{H2O} and temperatures, integration of Equation (7) leads to:

$$2 \cdot \left(1 - (1 - X_c)^{\frac{1}{2}}\right) = k_{SCM} \cdot t \qquad with \qquad k_{SCM} = A \cdot \exp\left(-\frac{E_a}{RT}\right) \cdot P_i^n. \quad (8)$$

This equation shows a linear evolution of $\left(1 - (1 - X_c)^{1/2}\right)$ with time. Figure 6(A) and (B) illustrate that, for the operating conditions used, the SCM represents the set of results. This result is in good agreement with other previous studies [5]. From the slope of the line, we determined the pre-exponential factor, the activation energy and the apparent reaction order which are equal to 69.8 $min^{-1}.Pa^{-n}$, 135 kJ/mol and 0.61, respectively. These values are consistent with other works in literature presented in Table 3 and in the review of Di Blasi [9].

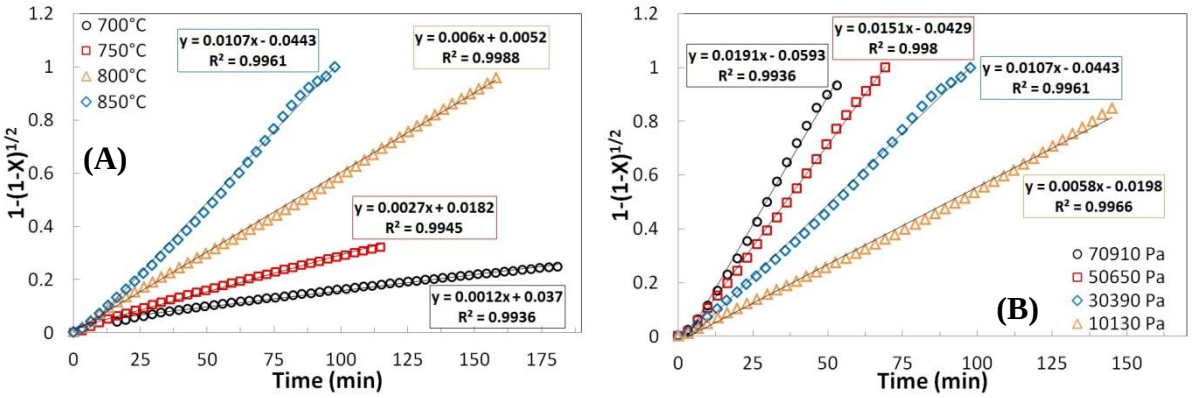

Figure 6 : Plot of the Shrinking Core Model and curve fitting parameters for steam gasification of the char at a total pressure of 1 atm, (A) at different temperatures and a steam partial pressure of 30390 Pa, (B) at various steam partial pressures and a temperature of 850°C.

Char type	*Temp.*	*Reactor*	*Ea*	*n*	*Model*	*Ref*
-	°C	-	kJ/mol	-	-	-
Victorian brown coal	650-1100	TGA	119-165	0.4-0.55	RPM	[4]
Coal Sub-bituminous	750-1100	Micro Fluidized bed	166	0.56-0.6	SCM	[5]
Lignite	880-980	Fixed bed	125.3	0.53	VM	[6]
Sub-bituminous	900-980		163.1	0.67	SCM	
Anthracite	920-1000		179.1	0.8	RPM	
Sawdust char	650-1000	TGA	198	0.75	SCM	[7]
Sawdust char	850-950	Fluidized bed	179	0.41	VM	[8]

Table 3 : Literature data for the steam gasification kinetics of coal and wood chars.

4. Conclusion

In this study, steam gasification of biomass chars were carried out in a fluidized bed reactor. Chars were obtained from fast pyrolysis of stick beech in a fluidized bed reactor at 650°C.

Char (STI650) were gasified in a fluidized bed reactor at temperatures between 700 and 850°C and steam partial pressure ranging from 10130 and 70910 Pa. It was shown that in the range of temperatures and steam partial pressures tested, gasification is subject to chemical control. Kinetic estimation resulted in activation energy of about 135 kJ/mol by using the Shrinking Core Model which was found to be the well-fitting model. The work also revealed that the reaction order with respect to the steam partial pressure was about 0.61.

Références

[1] C. Di Blasi, Modeling chemical and physical processes of wood and biomass pyrolysis, *Progress in Energy and Combustion Science*, 34(2008), 47-90.

[2] H. Hofbauer, R. Rauch, G. Loffler, S. Kaiser, Six years experience with the FICFB-gasification process, na. (2002).

[3] M. Morin, S. Pecate, M. Hémati, O. Marsan, Biomass gasification in a fluidized bed reactor: effect of temperature on properties and oxidative reactivity of chars, *5th International Congress on Green Process Engineering* (19-24 June 2016), na.

[4] J. Tanner, S. Bhattacharya, Kinetics of CO_2 and steam gasification of Victorian brown coal chars, *Chemical Engineering Journal*, 285(2016), 331-340.

[5] F. Wang, X. Zeng, Y. Wang, J. Yu, G. Xu, Characterization of coal char gasification with steam in a micro-fluidized bed reaction analyzer, *Fuel Processing Technology*, 141(2016), 2-8.

[6] Q. Yan, J. Huang, J. Zhao, C. Li, L. Xia, Y. Fang, Investigation into the kinetics of pressurized steam gasification of chars with different coal ranks, *J. Therm. Anal. Calorim*, 116(2014), 519-527.

[7] M. Hémati, C. Laguerie, Determination of the kinetics of the wood sawdust steam gasification of charcoal in a thermobalance, *Entropie*, 142(1988), 29-40.

[8] T. Kojima, P. Assavadakorn, T. Furusawa, Measurement and evaluation of gasification kinetics of sawdust char with steam in an experimental fluidized bed, *Fuel Processing Technology*, 36(1993), 201-207.

[9] C. Di Blasi, Combustion and gasification rates of lignocellulosic chars, *Progress in Energy and Combustion Science*, 35(2009), 121-140.

[10] Q. Xu, S. Pang, T. Levi, Reaction kinetics and producer gas compositions of steam gasification of coal and biomass blend chars, part 1: Experimental investigation, *Chemical Engineering Science*, 66(2011), 2141-2148.

[11] A. Gomez, R. Silbermann, N. Mahinpey, A comprehensive experimental procedure for CO2 coal gasification: is there really a maximum reaction rate?, *Applied Energy*, 124(2014), 73-81.

[12] A. Gomez, N. Mahinpey, Kinetic study of coal steam and CO_2 gasification: a new method to reduce interparticle diffusion, *Fuel*, 148(2015), 160-167.

[13] S.K. Bathia, D.D. Perlmutter, A random pore model for fluid-solid reaction: I. Isothermal, kinetic control, *AiChE Journal*, 26(1980), 379-386.

[14] C.Y. Wen, Noncatalytic heterogeneous solid fluid reaction models, *Industrial and Engineering Chemistry*, 60(1968), 34-54.